J. Chem. Sci. Vol. 126, No. 2, March 2014, pp. 429–435.

Facile synthesis of catalytically active CeO_2–Gd_2O_3 solid solutions for soot oxidation

D NAGA DURGASRI, T VINODKUMAR and BENJARAM M REDDY*

Inorganic and Physical Chemistry Division, CSIR-Indian Institute of Chemical Technology, Uppal Road, Hyderabad 500 607, India
e-mail: bmreddy@iict.res.in

MS received 9 September 2013; revised 20 December 2013; accepted 23 December 2013

Abstract. CeO_2–Gd_2O_3 oxides were synthesized by a modified coprecipitation method and subjected to thermal treatments at different temperatures to understand their thermal behaviour. The obtained samples were characterized by XRD, BET, TEM, Raman and TPR techniques. Catalytic efficiencies for oxygen storage/release capacity (OSC) and soot oxidation were evaluated by a thermogravimetric (TG) method. XRD and Raman results indicated the formation of $Ce_{0.8}Gd_{0.2}O_{2-\delta}$ (CG) solid solutions at lower calcination temperatures, and TEM studies confirmed nanosized nature of the particles. Raman studies further confirmed the presence of oxygen vacancies and lattice defects in the CG sample. TPR measurements indicated a facile reduction of ceria after Gd^{3+} addition. Activity studies revealed that incorporation of Gd^{3+} into the ceria matrix favoured the creation of more structural defects, which accelerates the oxidation rate of soot compared to pure ceria.

Keywords. Ceria–gadolinia; oxygen vacancies; reducibility; soot oxidation.

1. Introduction

In recent years, diesel engines have been prevalent power sources for vehicles owing to their superior efficiency, durability, and reliability in comparison with gasoline-powered vehicles. However, emission of toxic gases should be tackled before its wide utilization. One of the major pollutants in diesel exhaust is particulate matter (PM), mainly composed of soot.[1] Abatement of soot particles has become a topic of great concern due to its potential health risks such as mutagenic and carcinogenic activities and new environmental legislations on exhaust specifications.[2] This calls for efficient exhaust gas treatment systems in diesel engines. As a consequence, various emission–reduction technologies have been developed and among them, particle traps combined with oxidation catalysts to convert soot particles into gaseous products is one of the most efficient. Catalytic performance of soot oxidation generally depends on the contact efficiency between catalyst and soot particles. In general, transfer of active oxygen species from the catalyst to soot particle becomes relatively easier under tight contact conditions. Particularly, the ability of nanoparticles to adsorb and activate oxygen for these reactions is stronger than bigger particles.[3] In recent times, a good number of catalytic materials such as precious metals, transition metal oxides, rare earth oxides etc., have been proposed.[4,5] Nanosized ceria (CeO_2) is one of the most active catalytic materials in various aspects. Effectiveness of soot oxidation over ceria is due to its excellent redox property ($Ce^{4+} \leftrightarrow Ce^{3+}$), in which soot is oxidized by the surface 'active oxygen' from the catalyst which is then reoxidized by the gas phase oxygen. It is associated with its oxygen storage capacity (OSC) and the ease of formation of labile oxygen vacancies.[6] However, pure cerium oxide has poor thermal resistance and sinters rapidly above 873 K and thereby loses its crucial oxygen storage/release capacity. Instead of ceria alone, several studies indicate that doping of ceria with certain transition or rare earth metal (Zr, Fe, La, etc.,) cations partially improves thermal resistance. In addition, it improves redox properties, OSC and oxygen mobility of ceria within the framework.These characteristics are very important to enhance the participation of 'active oxygen' in oxidation processes.[6–9] Recently, Shen *et al*.[8] investigated iron-doped ceria for soot oxidation. According to their study, soot oxidation activity was improved by improvement of oxygen vacancies in the ceria matrix.

Over the last decade, our group has been actively engaged in the design of novel ceria-based material for various applications.[10] It has been established that incorporation of gadolinium into the ceria lattice greatly enhances the reducibility of Ce^{4+} in the catalyst material, which generated considerable interest about the

*For correspondence

Ce–Gd system. Substitution of Gd^{3+} in the ceria lattice could create structural defects, induce more surface active oxygen species, and accelerate oxygen diffusion,[11,12] since the charge and ionic radius are different from that of host ion. The present study was undertaken against the aforesaid background. To the best of our knowledge, Gd-containing ceria-based soot combustion catalysts have never been reported in open literature. In this study, gadolinium-doped ceria solid solutions were synthesized by a modified coprecipitation method and subjected to thermal treatments at different temperatures to evaluate catalytic efficiency of Ce-Gd-oxides towards soot oxidation. Synthesized materials were characterized by using X-ray diffraction (XRD), BET surface area, transmission electron microscopy (TEM), Raman spectroscopy (RS), and temperature programmed reduction (TPR) techniques. The main objective of this study was to investigate the relationship between physicochemical properties and catalytic activity, which will provide information about the key factors that control the activity.

2. Experimental

2.1 *Sample preparation*

The investigated $Ce_{1-x}Gd_xO_{2-\delta}$ (CG, x = 0.2) solid solutions were prepared by a modified coprecipitation method in a 20 g batch. In a typical procedure, to synthesize the CG sample, a 0.38 M solution was prepared by dissolving 33.05 g of cerium (III) nitrate (Aldrich, AR grade) in 200 mL of deionized water and a 0.18 M solution by dissolving 17.17 g of gadolinium (III) nitrate (Fluka, AR grade) separately in 200 mL deionized water and mixed together under stirring conditions for 1 h. Dilute aqueous ammonia was added dropwise until precipitation was complete and the solution mixture was diluted to 4000 mL with deionized water and stirred for 24 h.[13] After 3 days ageing, the obtained precipitates were filtered off, washed thoroughly until free from anion impurities, and dried at 393 K for 12 h. After grinding, the obtained sample was subsequently calcined at 773, 873, 973, and 1073 K for 5 h at a heating rate of 5 K min^{-1} in air atmosphere to obtain the final oxide materials. The obtained samples were labelled as CG 773, CG 873, CG 973, and CG 1073. For comparative purpose, pure cerium oxide was also prepared in a similar way.

2.2 *Characterization*

Powder X-ray diffraction data were acquired on a Rigaku multiflex diffractometer utilizing nickel-filtered Cu Kα (0.15418 nm) radiation source and a scintillation counter detector. The step size and the time per step were, respectively, fixed at 0.02° and 1 s in the range of $2 - 80°$. The mean crystallite size of the solid solution phases was estimated with the help of Scherrer equation from the line broadening, and the lattice parameter was calculated by a standard cubic indexation method using the intensity of most prominent peaks. Textural properties of the prepared samples were determined by N_2 adsorption–desorption isotherms at liquid N_2 temperature (77 K) on a Micromeritics (ASAP 2000) analyser via a thermal conductivity detector (TCD). Specific surface area and pore size distribution were calculated by Brunauer–Emmett–Teller (BET) and Barrett–Joyner–Halenda (BJH) methods, respectively. Prior to the measurements, the samples were pre-treated in vacuum at 473 K for 2 h to remove any residual moisture.

The TEM images were recorded on Philips CM200 and JEOL 2000EX electron microscopes with 0.23 and 0.21 nm point-to-point resolutions, respectively. For these studies, a suspension of the sample in ethanol was placed in an ultrasound bath and then a drop of it was supported on a holey carbon grid. The specimen was examined under vacuum at room temperature.

The Raman spectra were collected on a Horiba Jobin-Yvon HR800 Raman spectrometer equipped with a liquid-nitrogen cooled charge coupled device (CCD) detector and a confocal microscope.

The H_2-TPR was carried out in a tubular quartz reactor coupled to a TCD of a gas chromatograph (Shimadzu) and performed in a conventional apparatus by monitoring H_2 consumed. The sample (30 mg of fresh catalyst) was heated at a rate of 10 K min^{-1} from room temperature to 900 K in 20 mL min^{-1} flow of 5% H_2 in Ar. Hydrogen consumption during reduction was calculated by passing the effluent gas through a molecular sieve trap to remove the produced water and was analysed by gas chromatograph using TCD.

The OSC of the catalysts was determined by TG method by employing a commercial Netzsch TG-DTA (Luxx, STA, 409 PC, Germany) analyser under repeated thermal treatments in the temperature window of 573–1073 K. About 20 mg of the catalyst was used for the OSC measurements under dynamic conditions. Before the measurement, the samples were held in flowing air to 1073 K to remove residual water and other volatile organics and cooled to 423 K and again heated to 1073 K. Weight change during thermal treatments was monitored by TG. OSC of the catalyst is measured in terms of the amount of oxygen released during heat treatments from the obtained graph. Weight loss of the sample during the second stage of heat treatment

was used to measure the oxygen release properties. All heating and cooling rates were in the steps of 5 K min^{-1}.

2.3 *Activity measurements*

Catalytic activity for soot oxidation was determined by thermogravimetric (TG) method with a Mettler Toledo, TGA/SDTA 851e instrument. Activity measurements were performed with O_2 in 'close contact' (ground in agate mortar) conditions with catalyst–soot mixtures in 4:1 w/w ratio. The model soot used is Printex-U provided by Degussa. A weighed amount of sample was placed in a TG crucible and heated to 1273 K in 100 mL min^{-1} flow of air and the heating rate was 10 K min^{-1}.

3. Results and discussion

The XRD patterns of CG oxides calcined at different temperatures are illustrated in figure 1. For comparison purpose, pure ceria is also included. All the cata-lysts exhibited well-resolved X-ray diffraction peaks and are very similar to the pure ceria lines, which are indexed to (111), (200), (220), (311), (222), (400), and (420).[14–16] No diffraction peaks pertaining to gadolinium oxide were observed and the change in lattice parameter (table 1) is an additional evidence to confirm the substitution of Ce^{4+} ions by Gd^{3+}. A non-monotonous peak shifting was observed in the samples owing to stress relaxation, which is caused by α mismatch (mismatch of linear thermal expansion coefficients of CeO_2 and Gd_2O_3, as shown in figure 1b)[17] narrowing of peaks associated with the fluorite phase has been observed upon increase in calcination temperature implying a growth in the crystallite size and is estimated by Scherrer formula, which is in the range of 6.96 to 10.76 nm. In case of pure ceria, it is 8.9 to 32.5 nm.[10] In general, an increase in the crystallite size is expected with increase in calcination temperature due to crystallization. Interestingly, no such pronounced influence on the crystallite size of the doped ceria is observed compared to pristine ceria, since formation of solid solutions between Ce- and Gd-oxides retards crystallite growth. Calculated BET surface area of samples calcined at different temperatures is listed in table 1. From this, it is clear that when Gd_2O_3 is incorporated into CeO_2, the surface area increased and it is more for CG 773. At high calcination temperature, a systematic decline in the surface area was observed due to agglomeration. However, this is more in the case of pristine ceria in contrast to CG solid solution. Figure 2 shows the isotherms and pore size distribution curves of the CG samples. From the

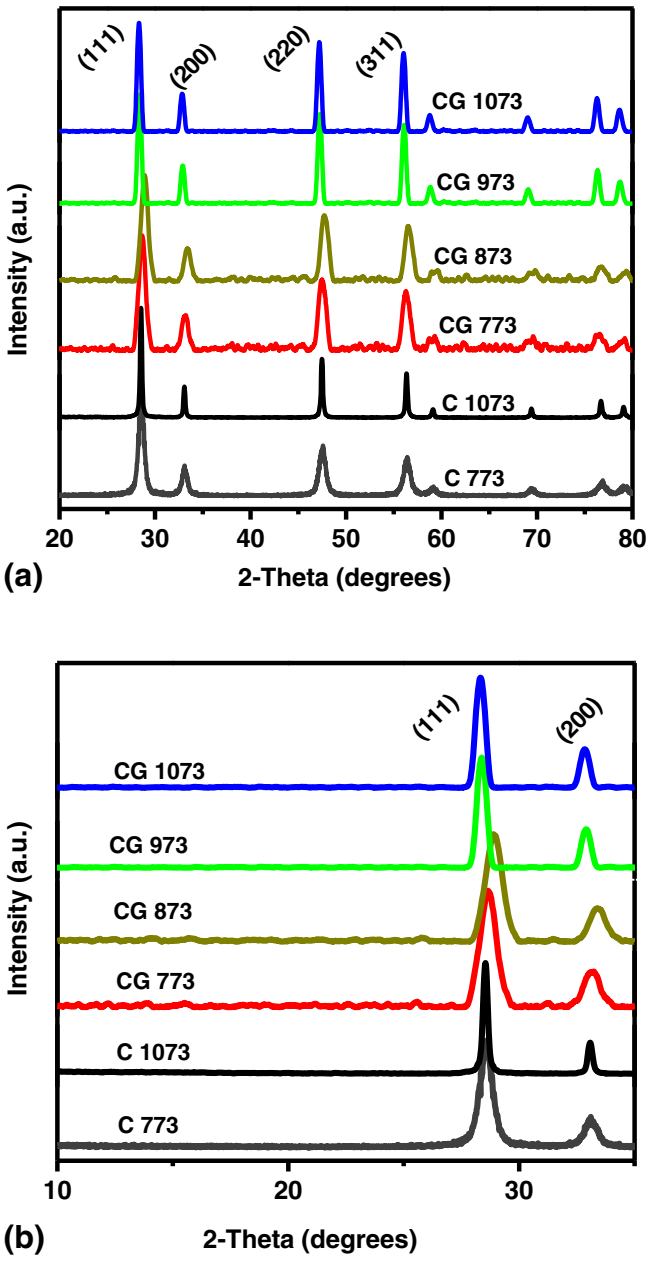

Figure 1. (**a**) Powder XRD patterns of ceria (C) and ceria–gadolinia samples (CG) calcined at various temperatures and (**b**) enlarged XRD patterns of the synthesized ceria (C) and ceria–gadolinia samples (CG) calcined at various temperatures.

relative pressure range, it is noticed that the obtained samples belong to type-IV isotherm, typical of mesoporous materials[18] and the BJH desorption cumulative pore volume for CG 773 is 0.17 cm^3 g^{-1}.

Figure 3 shows the TEM micrographs and selected area electron diffraction (SAED) patterns of CG catalysts calcined at 773 and 1073 K. The SAED patterns of these two samples show that both consisted of cubic ceria nanocrystals and had better crystallinity. It can be observed from the images that nanocrystals

Table 1. BET surface area, crystallite size and lattice parameter values of the prepared CeO_2–Gd_2O_3 (CG) oxides and ceria (C) calcined at different temperatures.

Sample	BET SA (m^2/g)	Crystallite size (nm)[a]	Lattice parameter (Å)[a]
C 773	41	8.9	5.410
C 1073	08	32.5	5.410
CG 773	74	6.96	5.412
CG 873	67	7.58	5.349
CG 973	41	9.49	5.439
CG 1073	37	10.76	5.440

[a] From XRD analysis

were uniformly dispersed and weekly aggregated and the average particle size calculated is consistent with XRD results.

Raman spectra of the CG solid solutions obtained with 632.81 nm laser line are shown in figure 4. Normally, pure ceria shows a sharp peak at 465 cm^{-1} ascribed to F_{2g} vibration of the fluorite type lattice and reveals the structure of symmetric breathing pattern of the oxygen atoms around Ce^{4+} ions.[19] However, a slight shift was observed from 465 cm^{-1} in pure ceria to 455.5 cm^{-1} in the mixed oxides, indicating decrease in particle size at the surface region. This may be due to the change in bond length, lattice spacing, and atomic geometry of ceria on doping. In addition to this main feature, the spectra showed two broad Raman bands at about 570 and 600 cm^{-1} (mentioned as α and β in figure 4) in the tail of the main band. These could be due to oxygen vacancies or structural defects introduced into the ceria lattice by two ways (i) to maintain charge neutrality when Ce^{4+} ions are replaced with Gd^{3+}(extrinsic vacancies) and (ii) intrinsic oxygen vacancies due to the presence of Ce^{3+} ions, respectively.[20,21] These distortions are important factors that help to explain high catalytic activities of these

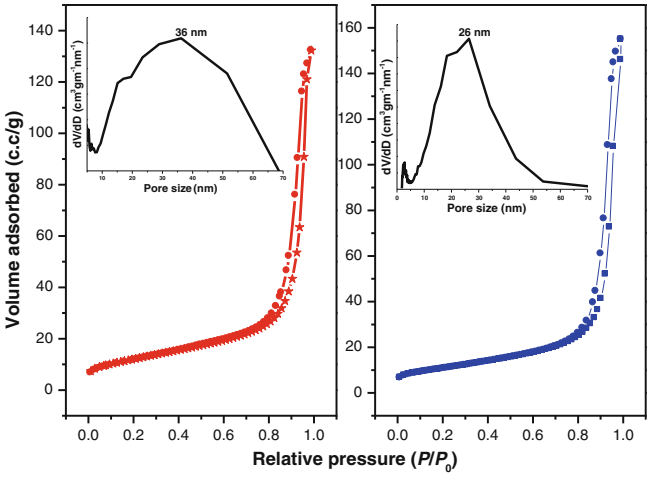

Figure 2. N_2 adsorption–desorption isotherms (Insets represent pore size distribution curves) of ceria–gadolinia samples calcined at 773 and 1073 K.

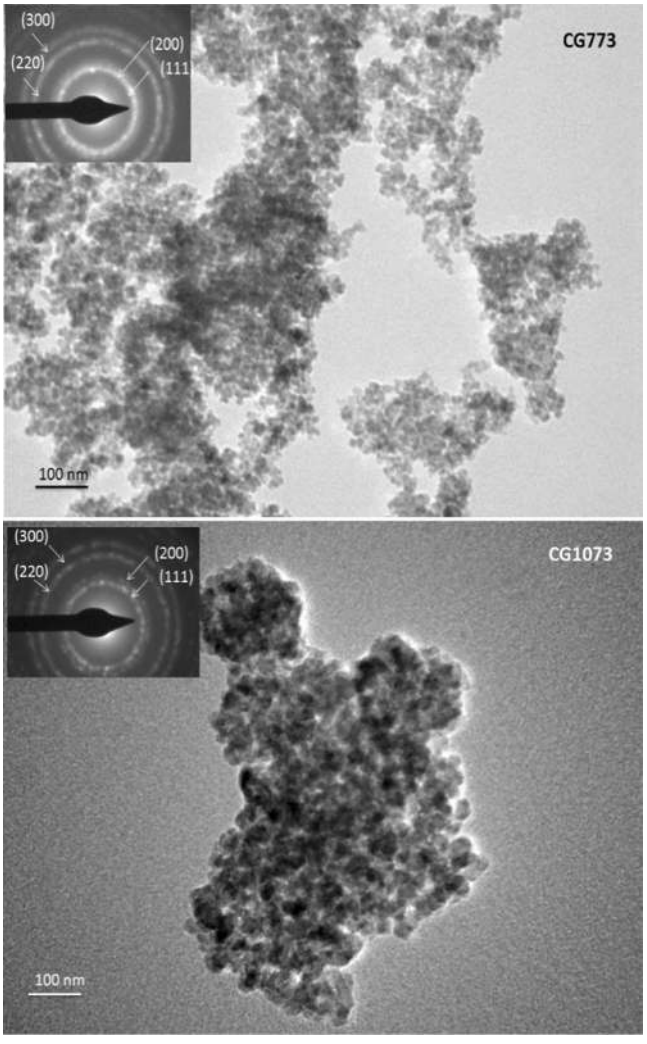

Figure 3. Transmission electron microscopy images of ceria–gadolinia (CG) samples calcined at 773 and 1073 K.

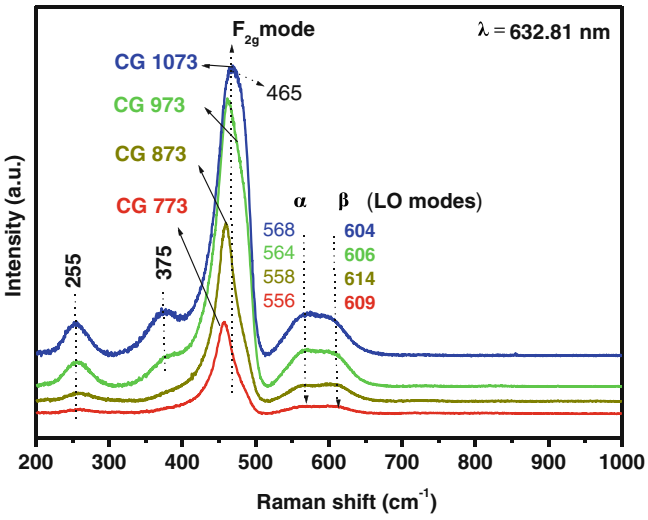

Figure 4. Raman spectra of ceria–gadolinia (CG) samples calcined at various temperatures.

materials in diesel soot oxidation. On the other hand, a vibrational mode for free Gd_2O_3 (band at 375 cm^{-1}) is observed for CG 1073 sample that reflects the influence of high temperature treatment.[21] Raman results indicate formation of oxygen vacancies even with the existing mixed phases of ceria and gadolinium.

Redox properties or catalytic ability of the synthesized samples were greatly improved by incorporation of gadolinium into ceria lattice. This can be understood from the TPR patterns. Figure 5 shows the evolution of H_2 consumption as a function of temperature for the prepared samples. Stepwise low-temperature (LT) and high-temperature (HT) reduction of pure ceria are typically identified at ~790 and 1070 K due to surface-capping of oxygen and bulk-phase lattice oxygen.[22] The pattern for these peaks is hard to distinguish in CG samples since high bulk oxygen mobility leads to a single peak formation and both surface and bulk reductions occur concurrently. Hence, a broad H_2-consumption peak was observed.[23,24] Results clearly show that formation of CeO_2–Gd_2O_3 solid solution with small crystallite size significantly improved reducibility of ceria. Here, peaks at around 795 and 844 K represent maximum H_2-consumption for CG 773 and CG 1073 samples. Observed difference between two catalysts is probably due to difference in concentration of oxygen vacancies, crystallite size and specific surface area.[25]

The OSC has been proven to be an imperative feature of soot combustion catalysts. OSC values of C 773, CG 773, and CG 1073 are 40, 168, 124 (μmol O_2/g ceria), respectively, as shown in figure 6. From this, it is clear that OSC of mixed oxides is higher than pure CeO_2 even at high calcination temperature. Since, defects created during incorporation of Gd^{3+} leads to ease of formation of labile oxygen vacancies, which facilitate relatively high mobility of bulk oxygen species within the lattice cell; thereby, enhancement in the OSC is detected. This property is responsible for improvement in redox nature of the material and thereby, increases 'active oxygen' species for oxidation process.[6]

Ceria has the potential to increase the soot oxidation rate by involving participation of 'active oxygen' and thereby lowers soot oxidation temperature. This is consistent with the fact that intrinsic Ce^{3+}/Ce^{4+} redox couple is responsible for the activity. Insertion of Gd_2O_3 into the CeO_2 lattice significantly improves the surface area, favours the creation of more 'active oxygen' species and accelerates the mobility of lattice

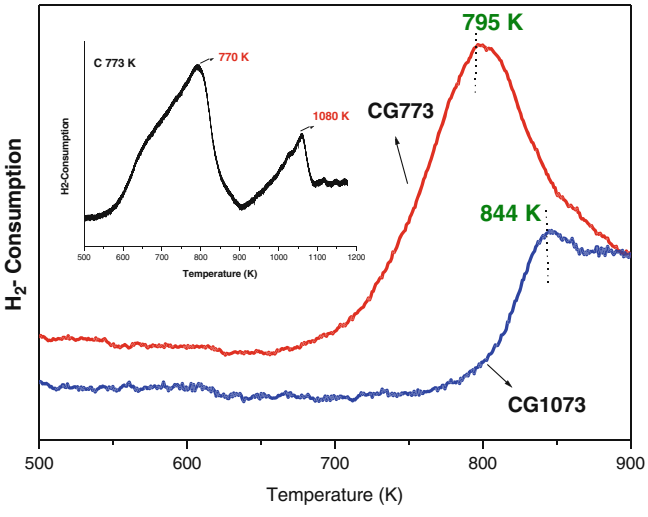

Figure 5. H_2-TPR profiles of ceria (C) and ceria–gadolinia (CG) samples calcined at different temperatures.

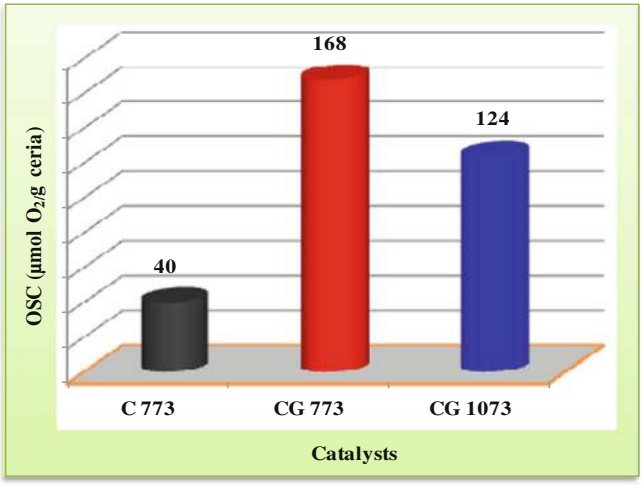

Figure 6. OSC profiles of ceria (C) calcined at 773 K and ceria–gadolinia (CG) samples calcined at 773 and 1073 K.

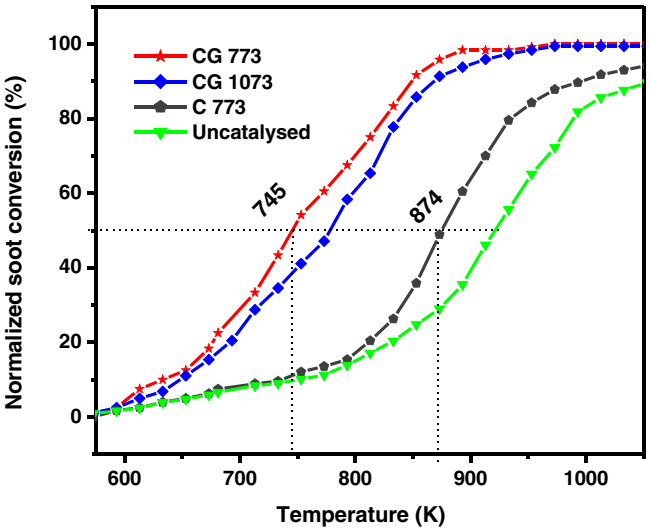

Figure 7. Normalized soot conversion (%) versus reaction temperature (K) of ceria (C) calcined at 773 K and ceria–gadolinia (CG) samples calcined at 773 and 1073 K along with uncatalysed soot.

oxygen.[26] Creation of such species starts at 600 K, thereby decreasing soot oxidation temperature. Under an intimate contact of soot and catalyst, active surface oxygen seems to be effectively transferred to soot surface and surface vacancy is replenished by the feed gas.[27] Soot combustion profiles over the prepared systems along with pure ceria and uncatalysed soot particles are shown in figure 7. Comparative performances of different catalysts for soot oxidation are usually established on the basis of their light-off temperatures (T_{50} = temperature at 50% conversion of soot). The best results were obtained for $Ce_{0.8}Gd_{0.2}O_{2-\delta}$-773 catalyst with T_{50} = 745 K, which is far less compared to bare ceria (T_{50} is 874 K) and uncatalysed soot (T_{50} = 920 K). Generation of 'active oxygen,' induced by Gd^{3+} explains high activity of CG catalysts in relation to CeO_2 alone. TG data along with the reducibility and OSC values support this observation. Bigger crystallite size and low specific surface area also seems to play a crucial role in decreasing soot oxidation with increase in calcination temperature.

4. Conclusion

Formation and structural modifications of CeO_2–Gd_2O_3 oxides were verified from XRD, TEM, Raman, and TPR. Gd^{3+} incorporation into CeO_2 provokes an increase in the OSC, which has a positive influence on catalytic activity. Soot oxidation is also highly dependent on surface area, crystallite size, and the extent of reducibility of the catalyst which are confirmed from the above results. As per the results of this study, two challenges remain for future research namely, creation of new materials that produce high amounts of active oxygen species and identification of suitable cations to dope into the CeO_2 lattice with a promising synthesis route. Further, it remains a challenge to design appropriate catalytic systems that improve contact efficiency between the soot and catalyst in order to favour constructive utilization of active oxygen.

Acknowledgements

DND and TV thank the Council of Scientific and Industrial Research (CSIR), New Delhi for the research fellowships. Financial support was received from the Department of Science and Technology, New Delhi, under SERB Scheme (SB/S1/PC-106/2012).

References

1. Wei Y, Liu J, Zhao Z, Duan A, Jiang G, Xu C, Gao J, He H and Wang X 2011 *Energy Environ. Sci.* **4** 2959
2. Simonsen S B, Dahl S, Johnson E and Helveg S 2008 *J. Catal.* **255** 1
3. Wei Y, Liu J, Zhao Z, Xu C, Duan A and Jiang G 2013 *Appl. Catal. A. Gen.* **453** 250
4. Liu J, Zhao Z, Chen Y, Xu C, Duan A and Jiang G 2011 *Catal. Today* **175** 117
5. Wei Y, Liu J, Zhao Z, Duan A and Jiang G 2012 *J. Catal.* **287** 13
6. Weng D, Li J, Wu X and Si Z 2011 *J. Environ. Sci.* **23** 145
7. Hensgen L and Stöwe K 2011 *Catal. Today* **159** 100
8. Shen Q, Lu G, Du C, Guo Y, Wang Y, Guo Y and Gong X 2013 *Chem. Eng. J.* **218** 164
9. Katta L, Sudarsanam P, Thrimurthulu G and Reddy B M 2010 *Appl. Catal. B Environ.* **101** 101
10. Reddy B M, Thrimurthulu G and Katta L 2011 *Catal. Lett.* **141** 572
11. Shan W, Ma N, Yang J, Dong X, Liu C and Wei L 2010 *J. Nat. Gas Chem.* **19** 86
12. Anjaneya K C, Nayaka G P, Manjanna J, Govindaraj G and Ganesha K N 2013 *J. Alloys Compoun.* **578** 53
13. Hernández W Y, Laguna O H, Centeno M A and Odriozola J A 2011 *J. Solid State Chem.* **184** 3014
14. Godinho M J, Gonçalves R F, S Santos L P, Varela J A, Longo E and Leite E R 2007 *Mat. Lett.* **61** 1904
15. Singh P, Mahadevaiah N, Parida S and Hegde M S 2011 *J. Chem. Sci.* **123** 577
16. Ranga Rao G and Sahu H R 2001 *J. Chem. Sci.* **113** 651
17. Sutradhar N, Sinhamahapatra A, Pahari S, Jayachandran M, Subramanian B, Bajaj H C and Panda A B 2011 *J. Phys. Chem.* **C115** 7628
18. Katta L, Vinod Kumar T, Durgasri D N and Reddy B M 2012 *Catal. Today* **198** 133
19. Guo M, Lu J, Wu Y, Wang Y and Luo M 2011 *Langmuir* **27** 3872
20. Li L, Chen F, Lu J-Q and Luo M-F 2011 *J. Phys. Chem.* **A115** 7972

21. Aškrabić S, Dohčević-Mitrović Z D, Radović M, Šcepanović M and Popović Z V 2009 *J. Raman Spectrosc.* **40** 650
22. Reddy B M, Thrimurthulu G, Katta L, Yamada Y and Park S-E 2009 *J. Phys. Chem. C.* **113** 15882
23. Li G-R, Qu D-L, Wang Z-L, Su C-Y, Tong Y-X and Arurault L 2009 *Chem. Commun.* **45** 7557
24. Dholabhai P P, Adams J B, Crozier P and Sharma R 2010 *Phys. Chem. Chem. Phys.* **12** 7904
25. Sun C, Li H and Chen L 2012 *Energy Environ. Sci.* **5** 8475
26. Fuentes R O, Muñoz F F, Acuña L M, Leyva A G and Baker R T 2008 *J. Mater. Chem.* **18** 5689
27. Wu X, Liu D, Li K, Li J and Weng D 2007 *Catal. Commun.* **8** 1274